

STUDIES ON THE GROWTH AND OPTICAL CHARACTERIZATION OF DYSPROSIUM PRASEODYMIUM OXALATE SINGLE CRYSTALS

V. Thomas^a, Anit Elizebeth^b, H. Thomas^a, G. Jose^b, N. V. Unnikrishnan^{b*}, Cyriac Joseph^b,
M. A. Ittyachen^b

^aDepartment of Physics, Christian College, Chengannur- 689 122, India

^bSchool of Pure and Applied Physics, Mahatma Gandhi University, Kottayam-686 560,
India

Preparation and optical characterization of dysprosium praseodymium oxalate (DPO) single crystals is reported. The crystals were grown by silica gel technique, by the controlled reaction of rare earth nitrates with oxalic acid. Crystals were characterized using X-ray powder diffraction, optical absorption and fluorescence studies. Radiative transition probability, fluorescence branching ratio and radiative lifetime of Dy³⁺ in the crystal are evaluated by the parameterization of the absorption spectrum by the Judd-Ofelt theory. The recorded fluorescence spectrum showed two well resolved peaks at 480 nm and 571 nm and are assigned to the transitions from ⁴F_{9/2}→⁶H_{15/2} and ⁶H_{13/2} of Dy³⁺. Stimulated emission cross-section and optical gain of these transitions are also evaluated.

(Received August 6, 2005; accepted September 22, 2005)

Keywords: Dy, Pr oxalate, Single crystal, Stimulated emission cross-section

1. Introduction

Visible lasers are widely used in the varied fields since the emergence of the first laser in 1960's. Blue-Green-red lasers can be realized by using LD or solid-state lasers. But a yellow laser in the range of 570-590 nm, which is very important in communication, military and commercial applications, has not been realized using LD or solid state lasers [1]. Trivalent rare earth ions have taken a dominant position as laser crystal activators responsible for stimulated emission in a variety of crystalline matrices. In fact laser action has been demonstrated in a variety of Dy³⁺ activated crystals [2]. Of the various family of the crystal hosts, oxalate crystals are of special significance due to their wide applicability in the development of miniature solid state lasers. The active ion concentration in this type of crystals can be of the order of 10²¹ ions/cm³, which encourages a high optical gain of the material. Since oxalates are insoluble in water and decompose before melting, growth by hydro-silica gel is the most suitable method for getting perfect crystals with minimum impurities and imperfections [3]. Mixed rare earth oxalates including cerium neodymium oxalate, cerium lanthanum oxalate [4], lanthanum samarium oxalate [5], neodymium praseodymium oxalate [6]. And lanthanum copper oxalate [7] have already been grown and reported. The purpose of the present study is to investigate the radiative properties of DyPr(C₂O₄)₃.10H₂O crystal and to predict its laser properties. Spectroscopic properties of rare earth ions in oxalate crystals have barely been investigated to our knowledge and hence the present study deserves special importance.

2. Experimental procedures

Single crystals of DPO were grown by the hydro silica gel method, which is widely accepted as the most suited techniques to grow oxalate crystals at room temperature. The growth was

* Corresponding author: spapf@sancharnet.in

accomplished by the controlled diffusion of gadolinium and dysprosium ions through silica gel impregnated with oxalic acid. The gel was prepared by mixing sodium meta silicate solution of desired specific gravity with 1M oxalic acid. An aqueous mixture of equal volume of praseodymium and dysprosium nitrate acidified with concentrated nitric acid was poured over the set gel. The outer electrolyte diffuses into the gel and the rare earth ions react with oxalate ions, which results in the crystallization of double oxalate crystals containing Pr^{3+} and Dy^{3+} ions.



The quality and size of the crystal vary depending on pH of the gel, concentration of the reactants and acidity of supernatant solution.. The optimum condition for the growth of well shaped good quality crystal is found to be pH 6 and gel density 1.04 gm/cc. Optical spectra of the crystals were recorded with UV-Visible spectrophotometer (Shimadzu UVPC 2401) and spectrofluorimeter (Shimadzu RFPC 5301). All the experiments were done at room temperature.

3. Results and discussion

3.1 Structural studies

Optical micrograph of the grown crystal is shown in Fig. 1. Morphology of the crystal varies from needle like to well faceted hexagonal with the concentration of the nitric acid incorporated in the supernatant solution. X-ray diffraction pattern of the grown samples of DGO crystals was recorded on a Philips model PW 1710 diffractometer with nickel filtered $\text{CuK}\alpha$ radiation ($\lambda = 1.5418 \text{ \AA}$) in the 2θ range $10-70^\circ$ and it is given in Fig. 2. The revelation of well-defined peaks establishes the crystalline nature of the sample. Since the ionic radii of gadolinium and dysprosium are comparable, one can expect identical crystal structure for DPO crystals as that of their single oxalate crystals. The similarity of the X-ray diffraction pattern of the DPO crystals with that of the corresponding single oxalate holds up this argument. The d-values of the DPO crystals are calculated and they are found to be comparable with the d-values of the single oxalates. The diffraction peaks were indexed assuming that DPO also crystallizes in the monoclinic system with space group $\text{P}2_1/\text{c}$ as in the case of their single component crystals. The close resemblance of the lattice parameters of DPO with that of praseodymium gadolinium oxalate and dysprosium oxalate support the assumption that the oxalate crystals containing two rare earths of comparable ionic radii can be formed by substitutional exchange of ions and are iso-structural with single oxalate crystals. The lattice parameters were evaluated and are given in Table 1.

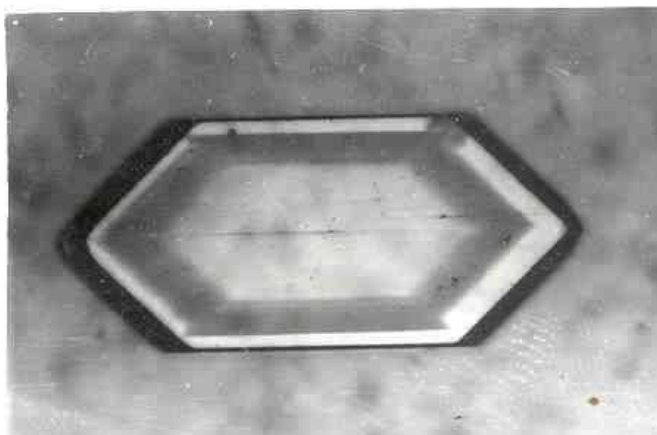


Fig. 1. Typical photograph of the GDO crystal.

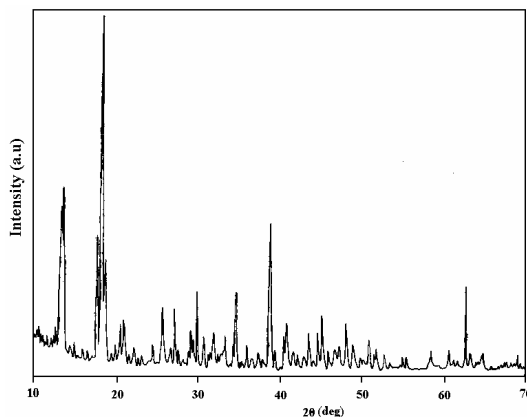


Fig. 2. X-ray diffraction pattern of the GDO crystal.

Table 1. Lattice parameters of GDO crystal.

| | |
|------------------|---|
| Chemical formula | GdDy(C ₂ O ₄) ₃ .10H ₂ O |
| Space group | P2 ₁ /C |
| A | 10.985 Å ⁰ |
| B | 9.598 Å ⁰ |
| C | 9.977 Å ⁰ |
| β | 114.14 ⁰ |

3.2 Optical studies

Room temperature absorption spectrum of the crystal is shown in Fig. 3. The energy level diagram of Dy³⁺ is given in Fig. 4. For Dy³⁺ ion all the transitions occur from ⁶H_{15/2} ground state. The strong absorption peak at around 250 nm is assigned to that of the oxalate group and the absorption peaks in the 400-450 nm range and at 540 nm are related to the transitions of Pr³⁺ ions (³H₄→³P₁, J= 0,1,2 and ³H₄→¹D₂) [1,8]. Intensities of all the absorption bands are evaluated by measuring their oscillator strengths (f), which are found to be proportional the area under the absorption line shapes. The experimental values of the oscillator strengths is expressed in terms of molar extinction coefficient (ε) and the energy of the transition in wave numbers (ν) by the following expression [8]

$$f = 4.32 \times 10^{-9} \int \epsilon(\nu) d\nu \quad (1)$$

where $d\nu$ is the band width at half height and (ε) the molar extinction coefficient at a given ν.

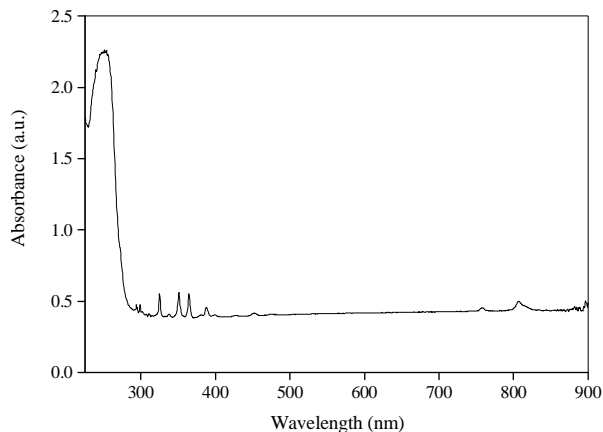


Fig. 3. Absorption spectrum of the GDO single crystal.

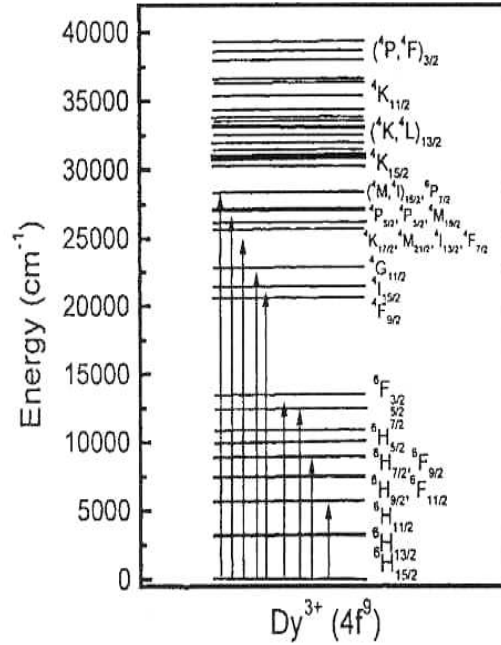


Fig. 4. Schematic diagram of the energy levels of Dy³⁺.

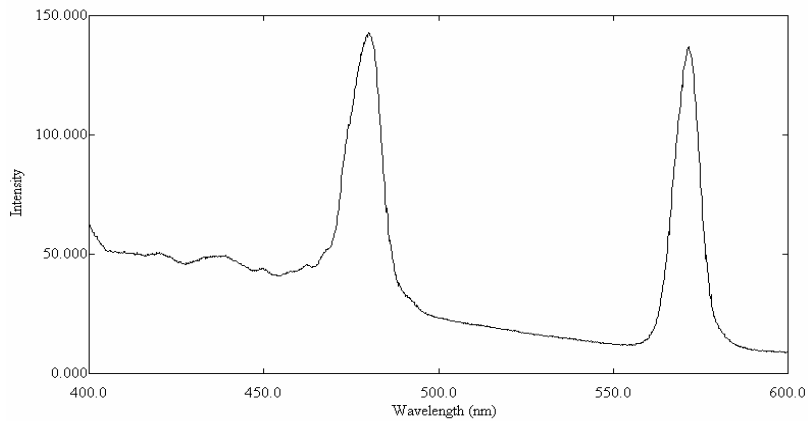


Fig. 5. Fluorescence spectrum of Dy³⁺ in GDO crystal.

Oscillator strengths can also be theoretically evaluated using the theory of Judd and Ofelt (JO) by assuming only the electric dipole contributions to the observed transitions [9-10]. To obtain reliable JO parameters a sufficient number of ground state transitions must be used. In practice five or six. Here Pr³⁺ has only four transitions in the region 200-900 nm and it is not possible to get reliable JO parameters of Pr³⁺ ion in the present DPO crystal [11]. Using the JO theory, the electric dipole line strengths S_{ed} can be found using the expression

$$S_{ed}(aJ, bJ) = e^2 \sum_{\lambda=2,4,6} \Omega_{\lambda} \langle \langle f^N[\alpha SL]J \| U^{\lambda} \| f^N[\alpha' S' L']J' \rangle \rangle \quad (2)$$

The squared reduced matrix elements $\|U^{\lambda}\|^2$ are calculated in the intermediate coupling case. As the variations in these squared reduced matrix elements are negligible from host to host, we have used the parameters given by Carnall et al [12]. The experimental oscillator strengths and electric dipole line strengths of the observed transitions are given in Table 2.

Table 2. Oscillator strengths and electric dipole line strengths of all the observed transitions ($\Omega_2=6.31 \times 10^{-20} \text{ cm}^2$, $\Omega_4=2.05 \times 10^{-20} \text{ cm}^2$, $\Omega_6=6.26 \times 10^{-20} \text{ cm}^2$).

| Transitions from | Energy ν (cm^{-1}) | f_{mes} (10^{-6}) | S_{ed} (10^{-20} cm^2) |
|-----------------------|-----------------------------------|--------------------------------|---|
| ${}^6\text{H}_{15/2}$ | | | |
| ${}^4\text{H}_{11/2}$ | 33444 | 0.3326 | 0.036 |
| ${}^6\text{P}_{3/2}$ | 31746 | 1.598 | 0.685 |
| ${}^4\text{I}_{9/2}$ | 30769 | 0.2592 | 0.0024 |
| ${}^6\text{P}_{7/2}$ | 29673 | 2.89 | 1.12 |
| ${}^6\text{P}_{5/2}$ | 28490 | 2.445 | 0.436 |
| ${}^4\text{F}_{7/2}$ | 27472 | 1.041 | 0.3189 |
| ${}^4\text{G}_{11/2}$ | 25773 | 0.1339 | 0.0733 |
| ${}^4\text{I}_{15/2}$ | 23474 | 0.589 | 0.467 |
| ${}^6\text{F}_{3/2}$ | 22123 | 0.447 | 0.385 |
| ${}^6\text{F}_{5/2}$ | 21097 | 3.047 | 2.27 |
| ${}^6\text{F}_{7/2}$ | 13175 | 0.112 | 4.26 |
| ${}^6\text{H}_{5/2}$ | 12376 | 0.596 | 0.016 |

Various radiative parameters viz, radiative transition probability (A), radiative life time (τ_{rad}), fluorescence branching ratio (β) of the active ion can be directly evaluated using the expressions

$$A[(S, L, J) : (S', L', J')] = \frac{64\pi^4 n \nu^3 (n^2 + 2)^2}{3h(2J + 1)} S_{\text{ed}} \quad (3)$$

$$\beta = \frac{A[(S, L, J) : (S', L', J')]}{\sum A[(S, L, J) : (S', L', J')]} \quad (4)$$

$$\tau_{\text{rad}} = \frac{1}{\sum A[(S, L, J) : (S', L', J')]} \quad (5)$$

The integrated absorption crosssection (Σ) for a particular transition is given by

$$\Sigma = \frac{1}{\nu^2} \frac{A}{8\pi c n^2} \quad (6)$$

Where A is the radiative transition probability, ν is the energy of the transition, c is the velocity of light and n is the refractive index of the medium.

The computed values of the A, A_T , β , τ_{rad} and Σ are summarised in Table 3.

 Table 3. Calculated radiative parameters of Dy^{3+} ion in the crystal.

| Transition from | Energy ν (cm^{-1}) | S_{ed} (10^{-22} cm^2) | A (s^{-1}) | A_T (s^{-1}) | τ_{rad} (μs) | β | σ_a (10^{-19} cm^2) |
|-----------------------|-----------------------------------|---|-----------------------|---------------------------|---------------------------------------|---------|--|
| ${}^6\text{F}_{1/2}$ | 7283 | 0.082 | 1 | 1609 | 622 | 0.0001 | 9.7 |
| ${}^6\text{F}_{3/2}$ | 7845 | 0.1878 | 1 | | | 0.0001 | 8.4 |
| ${}^6\text{F}_{5/2}$ | 8649 | 4.51 | 7 | | | 0.0045 | 48 |
| ${}^6\text{F}_{7/2}$ | 10082 | 0.3 | 8 | | | 0.0046 | 40 |
| ${}^6\text{H}_{5/2}$ | 10892 | 1.509 | 5 | | | 0.003 | 21 |
| ${}^6\text{H}_{7/2}$ | 11955 | 6.7561 | 29 | | | 0.018 | 10 |
| ${}^6\text{F}_{9/2}$ | 12039 | 1.9863 | 9 | | | 0.0053 | 42 |
| ${}^6\text{F}_{11/2}$ | 13361 | 4.5872 | 26 | | | 0.016 | 75 |
| ${}^6\text{H}_{9/2}$ | 13390 | 4.02 | 23 | | | 0.014 | 66 |
| ${}^6\text{H}_{11/2}$ | 15269 | 8.7 | 74 | | | 0.047 | 16 |
| ${}^6\text{H}_{13/2}$ | 17670 | 71.69 | 930 | | | 0.598 | 154 |
| ${}^6\text{H}_{15/2}$ | 21140 | 19.78 | 445 | | | 0.286 | 51 |

The stimulated emission crosssection has been measured for the different emission bands using the following expression

$$\sigma_e = \lambda_p^4 A / 8 \pi c n^2 \Delta\lambda \quad (7)$$

where λ_p is the peak wavelength of the emission band and $\Delta\lambda$ is the effective fluorescence bandwidth obtained by integrating the line shape and dividing by the peak intensity. Knowing the stimulated emission cross-section and the excited state population density (W), the gain coefficient $g(\lambda)$ can be evaluated using the expression [8]

$$g(\lambda) = N\lambda e \quad (8)$$

the gain $G(\lambda)$ is obtained from the expression

$$G(\lambda) = \exp(gl) \quad (9)$$

where 'l' is the exciting wavelength of the crystal.

The calculated stimulated emission crosssection effective bandwidth and optical gain are presented in Table 4. For Dy^{3+} in the present oxalate matrix two well resolved fluorescence bands at 480 nm and 571 nm (${}^4F_{9/2} \rightarrow {}^6H_{15/2}$ and ${}^6H_{13/2}$) are observed. The calculated stimulated emission cross-section and hence the optical gain values are maximum for ${}^4F_{9/2} \rightarrow {}^6H_{13/2}$ transition and can be exploited for optical amplifications in the oxalate matrix.

Table 4. Measured emission spectral datas of Dy^{3+} ion in the crystal.

| Fluorescence transition from ${}^4F_{9/2}$ | $\Delta\lambda$ | β | σ_e (10^{-21} cm ²) | G(λ) |
|--|-----------------|---------|---|----------------|
| ${}^6H_{13/2}$ | 9 | 0.598 | 1.23 | 3.73 |
| ${}^6H_{15/2}$ | 9 | 0.286 | 1.07 | 2.75 |

4. Conclusions

The DPO single crystals were grown for the first time and characterized using X-ray diffraction, optical absorption and fluorescence spectra. Determination of the unit cell parameters establishes that the mixed compound is iso-structural with its individual compounds gadolinium oxalate and dysprosium oxalate, which crystallize in monoclinic system. The radiative parameters are calculated using the Judd-Ofelt theory and the analysis shows that the ${}^4F_{9/2} \rightarrow {}^6H_{13/2}$ transition in the fluorescence spectrum can be exploited for optical amplification.

References

- [1] S. Shang, Z. Cheng, Z. Zhuo, T. Han, H. Chen, Phys. Stat.Solidii. (A) **181** 485 (2000).
- [2] P Babu, C. K Jayasankar, Opt Mater. **15** 65 (2000).
- [3] H. K. Henish, Crystal Growth In Gels, Pennsylvania University Press, Pennsylvania (1970).
- [4] M. V. John, M. A. Ittyachen, Cryst. Res. Technol **36** 141 (2001).
- [5] V John, M. A. Ittyachen, K. S. Raju, Bull. Mater. Sci. **20** 1059 (1997).
- [6] C. Joseph, G. Varughese, M. A. Ittyachen Cryst. Res. Technol **30** 151 (1995).
- [7] G. Varghese, M. A. Ittyachen, J. Issac Cryst. Res. Technol **25** 153 (1990).
- [8] G. A. Kumar, J. Phys. Chem. Solids **62**, 1327 (2001).
- [9] B. R. Judd, Phys. Rev. **127**, 750 (1962).
- [10] G. S. Ofelt, J. Chem. Phys. **37**, 511 (1962).
- [11] R. S. Quimby, W. J. Miniscallo, J. Appl. Phys. **75**, 614 (1994).
- [12] W. T. Carnaal, P. R. Fields, K. Rajnak, J. Chem. Phys. **49**, 4429 (1968).